

## PUBLICATION INFORMATION

This is the author's version of a work that was accepted for publication in the Continental Shelf Research journal. Changes resulting from the publishing process, such as peer review, editing, corrections, structural formatting, and other quality control mechanisms may not be reflected in this document. Changes may have been made to this work since it was submitted for publication. A definitive version was subsequently published in <https://doi.org/10.1016/j.csr.2018.10.008>

Digital reproduction on this site is provided to CIFOR staff and other researchers who visit this site for research consultation and scholarly purposes. Further distribution and/or any further use of the works from this site is strictly forbidden without the permission of the Continental Shelf Research journal.

You may download, copy and distribute this manuscript for non-commercial purposes. Your license is limited by the following restrictions:

1. The integrity of the work and identification of the author, copyright owner and publisher must be preserved in any copy.
2. You must attribute this manuscript in the following format:

This is a manuscript version of an article by Macklin, P.A., Suryaputra, I.G.N.A., Maher, D.T., Murdiyarto, D., Santos, I.R. 2019. **Drivers of CO<sub>2</sub> along a mangrove-seagrass transect in a tropical bay: Delayed groundwater seepage and seagrass uptake.** *Continental Shelf Research*, 172: 57-67

DOI: <https://doi.org/10.1016/j.csr.2018.10.008>



**Drivers of CO<sub>2</sub> along a mangrove-seagrass transect in a tropical bay: delayed groundwater seepage and seagrass uptake.**

Paul A. Macklin<sup>a, b\*</sup>, I Gusti Ngurah Agung Suryaputra<sup>b</sup>, Damien T. Maher<sup>a, b</sup>, Daniel Murdiyarso<sup>d, e</sup>, Isaac R. Santos<sup>a, b</sup>

<sup>a</sup> National Marine Science Centre, Southern Cross University, Coffs Harbour, New South Wales 2450, Australia.

<sup>b</sup> School of Environment, Science and Engineering, Southern Cross University, Lismore, New South Wales 2450, Australia.

<sup>c</sup> Department of Chemical Analysis, Faculty of Mathematics and Natural Sciences, Universitas Pendidikan Ganesha. Jl. Udayana no. 11 Singaraja, Bali 81116, Indonesia.

<sup>d</sup> Center for International Forestry Research (CIFOR), Jl. Situgede, Bogor 16115, Indonesia.

<sup>e</sup> Department of Geophysics and Meteorology, Bogor Agricultural University, Bogor 16680, Indonesia.

\* Corresponding author. Phone: +6287860331202 , Fax: +61 2 66212669. Email: paul.macklin@scu.edu.au

## Abstract

Water-to-air carbon dioxide fluxes from tropical coastal waters are an important but understudied component of the marine carbon budget. Here, we investigate drivers of carbon dioxide partial pressure ( $p\text{CO}_2$ ) in a relatively pristine mangrove-seagrass embayment on a tropical island (Bali, Indonesia). Observations were performed over eight underway seasonal surveys and a fixed location time series for 55 hours. There was a large spatial variability of  $p\text{CO}_2$  across the continuum of mangrove forests, seagrass meadows and the coastal ocean. Overall, the embayment waters surrounded by mangroves released  $\text{CO}_2$  to the atmosphere with a net flux rate of  $18.1 \pm 5.8 \text{ mmol m}^{-2} \text{ d}^{-1}$ . Seagrass beds produced an overall  $\text{CO}_2$  net flux rate of  $2.5 \pm 3.4 \text{ mmol m}^{-2} \text{ d}^{-1}$ , although 2 out of 8 surveys revealed a sink of  $\text{CO}_2$  in the seagrass area. The mouth of the bay where coral calcification occurs was a minor source of  $\text{CO}_2$  ( $0.3 \pm 0.4 \text{ mmol m}^{-2} \text{ d}^{-1}$ ). The overall average  $\text{CO}_2$  flux to the atmosphere along the transect was  $9.8 \pm 6.0 \text{ mmol m}^{-2} \text{ d}^{-1}$ , or  $3.6 \times 10^3 \text{ mol d}^{-1} \text{ CO}_2$  when upscaled to the entire embayment area. There were no clear seasonal patterns in contrast to better studied temperate systems.  $p\text{CO}_2$  significantly correlated with antecedent rainfall and the natural groundwater tracer radon ( $^{222}\text{Rn}$ ) during each survey. We suggest that the  $\text{CO}_2$  source in the mangrove dominated upper bay was associated with delayed groundwater inputs, and a shifting  $\text{CO}_2$  source-sink in the lower bay was driven by the uptake of  $\text{CO}_2$  by seagrass and mixing with oceanic waters. This differs from modified landscapes where potential uptake of  $\text{CO}_2$  is weakened due to the degradation of seagrass beds, or emissions are increased due to drainage of coastal wetlands.

Keywords: blue carbon; submarine groundwater discharge; greenhouse gas emissions; mangrove forests; seagrass beds; ecosystem connectivity.

## **1. Introduction**

The large net primary production of the world's coastal embayments are exported to coastal waters (Robertson et al., 1992) primarily through the interplay of tidal dynamics and seasonal river discharge. With a global area of  $\sim 45000 \text{ km}^2$ , intertidal areas of temperate embayments predominantly comprise of salt marsh habitats (Greenberg et al., 2006) occupying low-lying topographic zones (Scott et al., 2014) and high distributions of seagrass beds in subtidal zones (Short et al., 2007). In contrast, tropical coastal embayments typically consist of a continuum of fringing coral reefs, seagrass beds and mangrove forests (Torres-Pulliza et al., 2013). Near-shore tropical mangrove forests are the most carbon-rich forests on earth, storing and sequestering globally significant amounts of carbon in their soils (Donato et al., 2011). Occupying only 0.02% of global surface area, mangrove forests are responsible for approximately 11% of the total terrestrial organic carbon delivery to oceans (Jennerjahn & Ittekkot, 2002; Sippo et al., 2017). Mangroves are tightly connected with their adjacent habitats (Signa et al., 2017) and support marine biodiversity, regulate water quality and protect tropical coastlines against storms (Ganguly et al., 2017).

Tropical seagrass beds are located shoreward of coral reefs and seaward of mangrove forests in areas with high light availability and favourable water quality (Guannel et al., 2016) and have been reported to be largely net autotrophic (i.e. a net atmospheric  $\text{CO}_2$  sink) (Duarte & Cebrian, 1996). Coastal geomorphology is recognised as being important in seagrass abundance, distribution and diversity, as these habitats usually exist near fringing reefs in protected, shallow coastal lagoons (Torres-Pulliza et al., 2013). Combined, mangrove forests and seagrass beds play a major role in biological connectivity of coastal embayments, acting as coastal buffers by filtering sediment and nutrient loads to adjacent coral reefs (Hemminga & Duarte, 2000).

Indonesia, lying between latitudes 6 °N and 11 °S, has a coastline of more than 95,180 km, the second longest coastline in the world (Spalding et al., 1997) and 2.9 Mha of mangrove cover, larger than any continent on earth (Atwood et al., 2017). With such an extent and high carbon stocks, Indonesia's mangrove forests store on average 3.14 PgC (Murdiyarso et al., 2015). However, in three decades (1985-2005), Indonesia has lost 40% of its mangroves, mainly as a result of aquaculture development (Giri et al., 2011). This has resulted in potential global annual emissions of 0.07 to 0.21 Pg CO<sub>2</sub> (Murdiyarso et al., 2015). Seagrass beds cover an estimated 30,000 km<sup>2</sup> of Indonesian coastline (Green & Short, 2003), and combined with mangrove forests, account for approximately 3.4 Pg C (~17%) of the global blue carbon reservoir (Alongi et al., 2016).

Mangrove-seagrass connectivity research has usually centred on the exchange of dissolved organic carbon (DOC) and particulate organic carbon (POC) (Dittmar et al., 2009; Hemminga et al., 1994; Maher et al., 2013; Müller et al., 2015). Little is known about CO<sub>2</sub> interactions between near-mangrove forest surrounding waters (described as mangrove forest water from here on) and adjacent seagrass beds. Stable isotope studies show that seagrasses close to mangroves have a more depleted  $\delta^{13}\text{C}$  value than those further away (Bouillon, Connolly, et al., 2008; Hemminga et al., 1994), suggesting that seagrasses are fixing DIC sourced from mangrove respiration.

Mangrove groundwater and porewater exchange can be an important source of carbon to coastal waters (Bouillon et al., 2007; Maher et al., 2013; Maher et al., 2017; Sadat-Noori et al., 2016). A recent literature review demonstrates that groundwater fluxes in mangroves can be a major component of tropical coastal carbon budgets with fluxes on the same order of magnitude as rivers (Chen et al., 2018). Since mangrove forests usually coexist with seagrass beds and coral reefs (Fourqurean et al., 1992), and carbon exchange along this continuum supports cross-productivity (Unsworth et al., 2008), understanding the relationship between

groundwater seepage, carbon dynamics and ecosystem connectivity in transition zones is important.

Here, we investigate the drivers of  $p\text{CO}_2$  dynamics along a mangrove-seagrass transect in Bali, Indonesia. We performed coupled, automated seasonal  $p\text{CO}_2$  and radon ( $^{222}\text{Rn}$ ; a natural groundwater tracer) investigations to assess whether  $\text{CO}_2$  is derived from groundwater or porewater pathways. We investigate temporal and spatial scales of  $p\text{CO}_2$  dynamics, hydrological drivers such as groundwater seepage, delayed antecedent rainfall, and interplay along the mangrove-seagrass continuum in a non-impacted embayment.

## **2. Material and methods**

### **2.1 Area description**

Gilimanuk Bay, a 3.7 km<sup>2</sup> coastal embayment, is located in Jembrana Regency on the northwest coast of Bali, Indonesia. Including two small islands, Kalong Island and Burung Island, the area contains some of Bali's most pristine mangrove forests (Thoha, 2007) (Figure 1). Oceanic upwelling and tidal exchange from the deep Java Strait supply nutrients to Gilimanuk Bay (Ningsih et al., 2013; Siswanto, 2008). The average depth of the embayment is ~2m, with intertidal zones in the upper embayment unnavigable at low tides (<0.5m; Figure 1). Patchy coral reefs are present in the channel at the ocean mouth of the embayment, while the lower and upper embayment consists of seagrass beds and sand flats. Due to the low-lying topography and geometry, predominant southeast winds (June-September) and northeast winds (December-March) produce small wind-generated waves (<0.5m), which influence the mangrove forest water in the upper embayment. Microtides with an average range of ~1 m occur in the bay, preventing significant current-driven turbulence. The bordering West Bali National Park on the northern side is comprised of mangrove forests (310 ha), lowland rain forest, savanna and sea grasses (40 ha), coral reefs (810 ha) and both

shallow and deep sea waters (3,520 ha) (Utama, 2015). The regional geology includes alluvial deposits and Prapat Agung Formation which consists of limestone, calcareous sandstone and marls (Purbo-Hadiwidjojo, 1971). Soils are hydromorphic alluvial in the near-shore zone and grey-brown alluvial surrounding the embayment. Dominant mangrove species in Gilimanuk Bay include *Rhizophora apiculata*, *Excoecaria agallocha*, and *Ceriops tagal* (Marbawa et al., 2015). Twelve of the world's sixty known species of seagrass are present in West Bali National Park (Purnomo et al., 2017). Dominant seagrass species include *Cymodocea rotundata*, *Halophila ovalis* and *Enhalus acoroides* (Purnomo et al., 2017; Zulkarnaen et al., 2014).

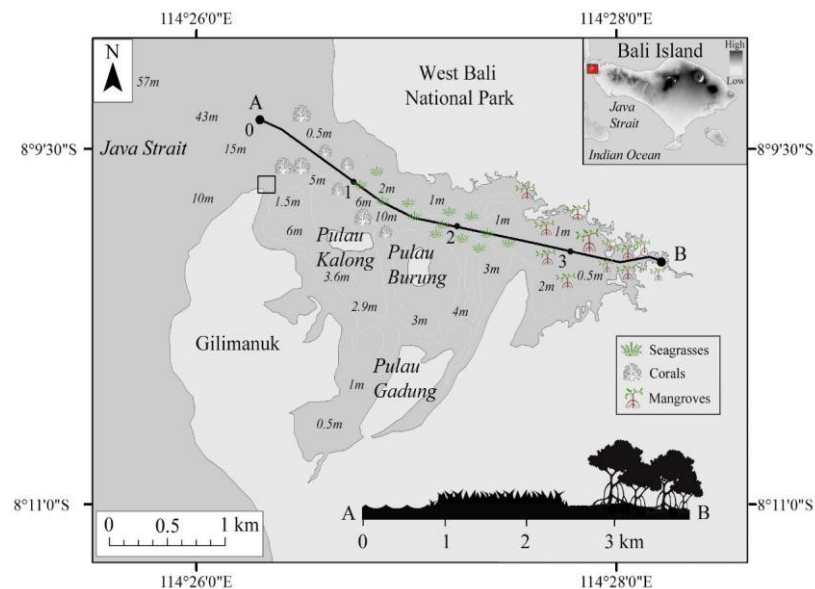


Figure 1. Gilimanuk Bay study site in western Bali. The A to B line and 0 to 3 along the line indicates the seasonal underway sampling route and distance travelled, respectively. The square near the mouth shows the location of the time series deployment. The location of seagrass beds and mangroves is indicated for the line A-B on the bottom right.

## 2.2 Approach and methods

To investigate hydrologic variations, groundwater seepage and CO<sub>2</sub> fluxes, we combined

eight underway spatial surveys (S1-S8) with a detailed 55 hour fixed location time series (TS) in Gilimanuk Bay between 20<sup>th</sup> November 2015 and 15<sup>th</sup> November 2017 (see Table 1). The average tidal range throughout the surveys was 1.3m. As S1 was conducted at the end of a subsequent drought period and followed by a period of prolonged rainfall, following surveys (S2-S8) were intended to replicate rainfall events and possible groundwater relationships. . During the underway surveys, we measured high resolution spatial variations at 10 minute intervals while location was tracked and logged by a Garmin GPS72 continuously. Each survey commenced at high tide beginning at the ocean mouth and ending upstream at the mangrove forest, in a small research vessel travelling between 4 and 6 km/hr, while the time series was conducted at the ocean mouth (Figure 1).

A Li-820 CO<sub>2</sub> detector and a radon-in-air monitor (RAD7, Durridge) were deployed to measure  $p\text{CO}_2$  and <sup>222</sup>Rn concentrations at approximately 1m depth. The Li-820 and the RAD7 were connected with a closed-air-loop to a shower head gas exchange (Dulaiova et al., 2005; Santos et al., 2012) using the methodology of Santos et al. (2012) and references therein. A Li-820 (calibrated before underway surveys with 0, 400 and 10 000 ppm spans) was checked for accuracy alongside a calibrated Li-820 which was deployed in the 55 hr time series at the end of the study campaign. The RAD 7 was, pre-calibrated by the manufacturer (Durridge) and is expected to hold calibration for at least one year. Mole fraction measurements provided by the Li-820 CO<sub>2</sub> detector were later calculated to  $p\text{CO}_2$  according to the recommendations of Pierrot et al. (2009). Atmospheric  $p\text{CO}_2$  was assumed to be constant at 400  $\mu\text{atm}$ . A Hydrolab DS-5 water quality sonde was calibrated before each survey and deployed to measure temperature, salinity and dissolved oxygen at 10 min intervals. We used a calibrated handheld YSI EcoSence EC300 meter and a Hatch 40D LDO Sensor for field measurements every 10 to 15 minutes, which were comparable to the Hydrolab DS-5 measurements.



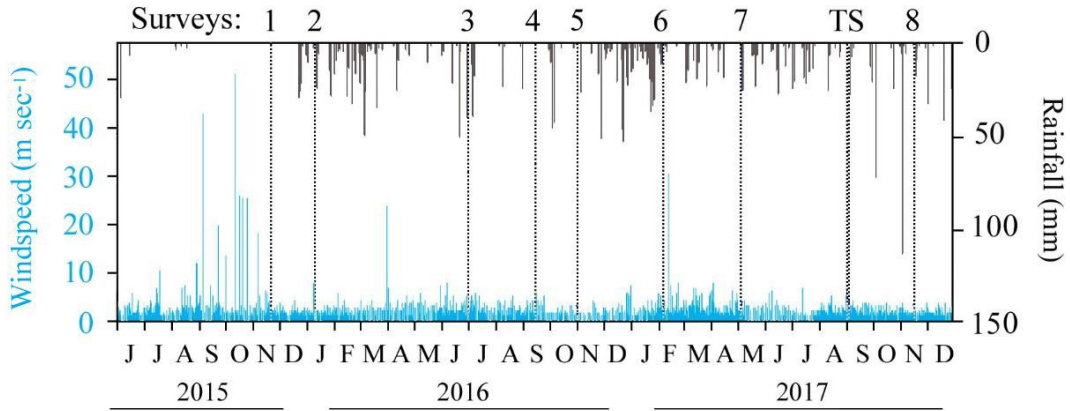


Figure 2. Daily rainfall including timing of the 8 underway surveys and a time series (TS; both vertical dotted lines) at the Gilimanuk ocean mouth from November 2016 to November 2017. Rainfall (black) and wind data (blue) were sourced from Banyuwangi Weather Station (8.21700°S, 114.38300°E; average atmospheric pressure=1021.5 hPa (1.0 atm); 10 m above sea level).

CO<sub>2</sub> fluxes at the water-air interface were then calculated as function of air-water CO<sub>2</sub> gradient ( $\Delta p\text{CO}_2$ ), temperature and salinity dependant solubility ( $k_0$  (Weiss, 1974)) and gas transfer velocity ( $k$ ) according to:

$$F_{\text{CO}_2} = k \cdot k_0 \Delta p\text{CO}_2,$$

where  $k$  is the CO<sub>2</sub> gas transfer velocity,  $K_0$  is the solubility of CO<sub>2</sub> (Weiss, 1974) and  $\Delta p\text{CO}_2$  is the difference between sea and air ( $p\text{CO}_{2\text{sea}} - p\text{CO}_{2\text{air}}$ ).

To calculate  $k$ , we used four wind-speed based parameterizations which provide a reasonable range in evasion rate estimates.

$$k = 0.0283u^3 (Sc/660)^{-1/2} \quad \text{Wanninkhof and McGillis (1999)} \quad (2)$$

$$k = 1.91e^{0.35u} (Sc/600)^{-1/2} \quad \text{Raymond and Cole (2001)} \quad (3)$$

$$k = 5.141u^{0.758} (Sc/600)^{-1/2} \quad \text{Borges et al. (2004)} \quad (4)$$

$$k = 0.251u^2 (Sc/660)^{-1/2} \quad \text{Wanninkhof (2014)} \quad (5)$$

where  $k$  is the transfer velocity ( $\text{cm h}^{-1}$ ),  $u$  is the wind speed ( $\text{ms}^{-1}$ ) at a height of 10m and  $Sc$  is the Schmidt number of  $\text{CO}_2$  at in situ temperature and salinity (Wanninkhof, 2014).

Positive  $\text{CO}_2$  flux values signify a  $\text{CO}_2$  exchange from water-to-air ( $\text{CO}_2$  source) while negative  $\text{CO}_2$  flux values signify an exchange from air-to-water ( $\text{CO}_2$  sink). Estimations of  $\text{CO}_2$  fluxes were calculated by using 10 minute sampling times for both underway and time series measured  $p\text{CO}_2$  data and average wind speeds from 28 days prior to each survey and the time series (Table 1). Rainfall and wind data were sourced from Banyuwangi Weather Station ( $8.21700^\circ\text{S}$ ,  $114.38300^\circ\text{E}$ ; average atmospheric pressure= $1021.5$  hPa ( $1.0$  atm); 10 m above sea level) located 7 km from the study site ([www.dataonline.bmkg.go.id](http://www.dataonline.bmkg.go.id)).

Table 1. Date, start and finish times (24hrs), tidal ranges (m), windspeeds ( $\text{m sec}^{-1}$ ) 24hrs, 48hrs, 7 days, 14 days and 28 days prior, for each survey (S1-S8) and the time series (TS) at the ocean mouth of the embayment.

Survey	Date	Start (24 hrs)	Finish (24 hrs)	Tidal range (m)	Windspeed (m/sec)				
					24 (hrs)	48 (hrs)	7 (days)	14 (days)	28 (days)
S1	20/11/2105	15:10	18:00	1.1	2.2	2.2	2	1.8	2
S2	9/01/2016	9:58	13:50	0.9	1.4	1.1	1.3	1.3	1.6
S3	30/06/2016	6:45	10:25	1.4	1.3	1.2	1.3	1.3	1.3
S4	14/07/2016	8:25	12:40	1.3	1.1	0.9	0.9	0.8	0.9
S5	30/10/2016	9:50	13:40	1.6	3.7	2.1	1.7	1.6	1.4
S6	15/02/2017	12:25	16:20	2.0	1.4	1.7	1.3	1.4	1.4
S7	5/05/2017	6:40	10:25	0.6	1.3	1	1.2	1.2	1.1
S8	15/11/2017	8:00	12:00	1.1	1.2	1.1	1.4	1.2	1.4
TS	31/08/2017	16:25	03/09/2017 at 1:20	1.5	2.1	1.7	1.5	1.6	1.5

### 3. Results.

#### 3.1 Seasonal spatial surveys

Water temperature was lowest at the ocean mouth increasing towards the shallow mangrove forest water endmember (max=34.7 °C; Table 2) throughout the eight underway surveys. The lowest salinity was observed in the mangrove forest water endmember (26.2; Survey 1) however overall average salinity ranges were relatively close to seawater (31.5 - 33.0) reflecting the characteristics of an ocean dominated embayment. Dissolved oxygen (DO) was slightly undersaturated at the ocean entrance and increased significantly in the seagrass beds in 5 out of 8 surveys (reaching 166.3 %; Survey 5, Figure 3), while the lowest DO was observed in the mangrove forest water area ( $\leq 60\%$  in 5 surveys). There was minimal tidal variation on survey days (mean= ~1.3m although Survey 6 tidal range was ~2m).

Table 2. Mean, standard deviation, minimum and maximum for  $p\text{CO}_2$ , radon, DO, salinity and temperature for eight underway spatial surveys and time series in Gilimanuk Bay.

		$p\text{CO}_2$ ( $\mu\text{atm}$ )	$^{222}\text{Rn}$ (dpm/L)	DO (%)	Salinity	Temp. (°C)
Survey 1	Mean	516	2.3	101	32.2	30.8
20-Nov-15	St. Dev $\pm$	207	1.5	15	2.9	1.2
	Min	294	0.2	82	26.2	28.9
	Max	930	4.2	121	34.8	32.5
Survey 2	Mean	1018	3.4	87	32.3	31.2
9-Jan-16	St. Dev	441	2.1	21	0.1	1.2
	Min	390	0.6	46	31.9	28.9
	Max	1750	6.0	126	32.5	32.5
Survey 3	Mean	796	2.6	87	31.5	30.7
30-Jun-16	St. Dev $\pm$	512	1.9	29	0.8	1.5

	Min	360	0.1	60	30.2	28.3
	Max	1965	5.9	140	33.0	32.9
Survey 4	Mean	908	2.0	77	32.7	26.5
14-Sep-16	St. Dev ±	385	1.5	9	1.1	1.7
	Min	399	0.1	60	31.1	23.8
	Max	1388	4.7	90	34.8	29.9
Survey 5	Mean	573	2.3	96	32.8	28.2
30-Oct-16	St. Dev ±	288	1.4	29	1.2	2.6
	Min	182	0.2	70	30.4	25.8
	Max	1167	4.4	166	33.9	33.9
Survey 6	Mean	1164	2.7	77	32.5	27.1
5-Jan-17	St. Dev ±	597	2.6	13	1.3	1.1
	Min	410	0.0	56	29.4	25.4
	Max	2101	7.4	96	34.7	28.8
Survey 7	Mean	560	0.9	85	33.1	29.8
5-May-17	St. Dev ±	214	0.6	11	1.1	1.9
	Min	399	0.1	69	31.6	27.4
	Max	1001	1.9	100	34.8	34.7
Survey 8	Mean	849	2.2	86	33.0	27.3
17-Nov-17	St. Dev ±	519	1.6	21	0.7	1.6
	Min	316	0.1	59	32.1	25
	Max	1600	4.9	141	34.5	30.6
Time Series	Mean	458	0.8	94	35.0	26.6
	St. Dev ±	17	0.7	4	0.1	0.7
	Min	425	0	83	34.9	25.1
	Max	514	3.1	104	35.2	27.7

---

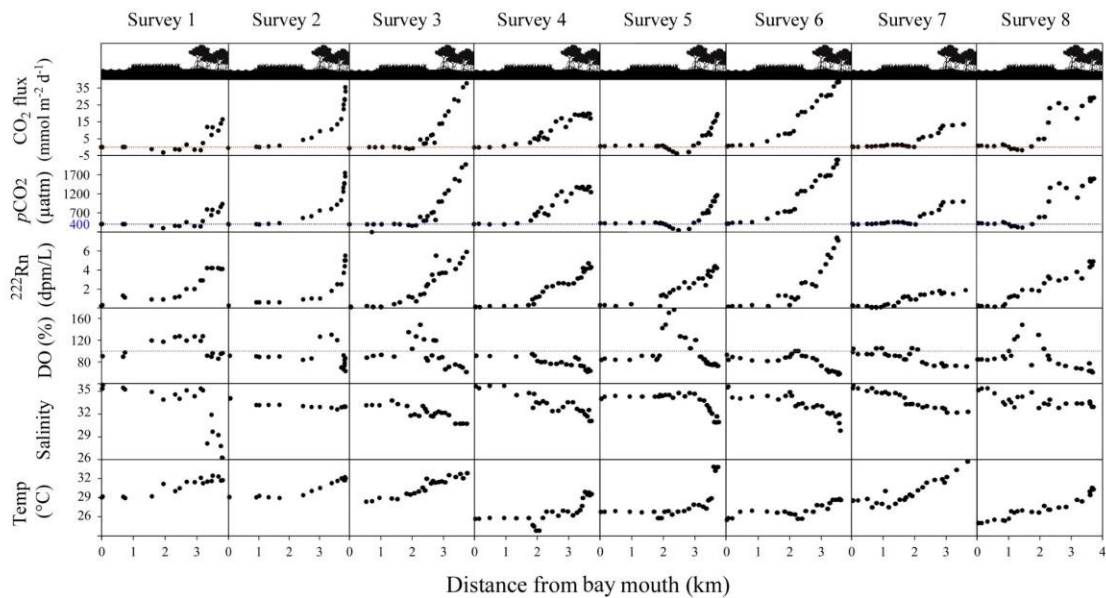


Figure 3. Distance plots for 8 underway seasonal surveys for CO<sub>2</sub> fluxes from the parameterization of Raymond and Cole (2001) (red line = source/sink boundary), pCO<sub>2</sub> measurements (blue line represents atmospheric pCO<sub>2</sub> concentrations ~400 μatm), <sup>222</sup>Rn, DO (grey line = 100% supersaturation), salinity and temperature from the ocean mouth of Gilimanuk Bay to the mangrove forest water.

<sup>222</sup>Rn (groundwater tracer) was lowest (0.1 dpm/L) at the ocean entrance and increased markedly towards the mangrove forest water where concentrations reached 7.4 dpm/L.

Stronger correlations between  $^{222}\text{Rn}$  and  $p\text{CO}_2$  than between dissolved DO and  $p\text{CO}_2$  (Figure 4) in 7 out of 8 surveys suggest that the seepage of groundwater, not pelagic respiration and photosynthesis, drove  $p\text{CO}_2$  supersaturation within the embayment, particularly in the mangrove forest water (Figure 4).  $p\text{CO}_2$  was mostly above atmospheric equilibrium ( $>400$   $\mu\text{atm}$ ) with up to a five-fold increase in the mangrove forest water (max = 2101  $\mu\text{atm}$ ). On average,  $p\text{CO}_2$  in the mangrove forest water was ~four-fold that of the overall embayment (Figure 3). In contrast, the seagrass beds were undersaturated in 30% of surveys suggesting that, seagrass was fixing mangrove water-derived  $\text{CO}_2$  from the upper embayment.

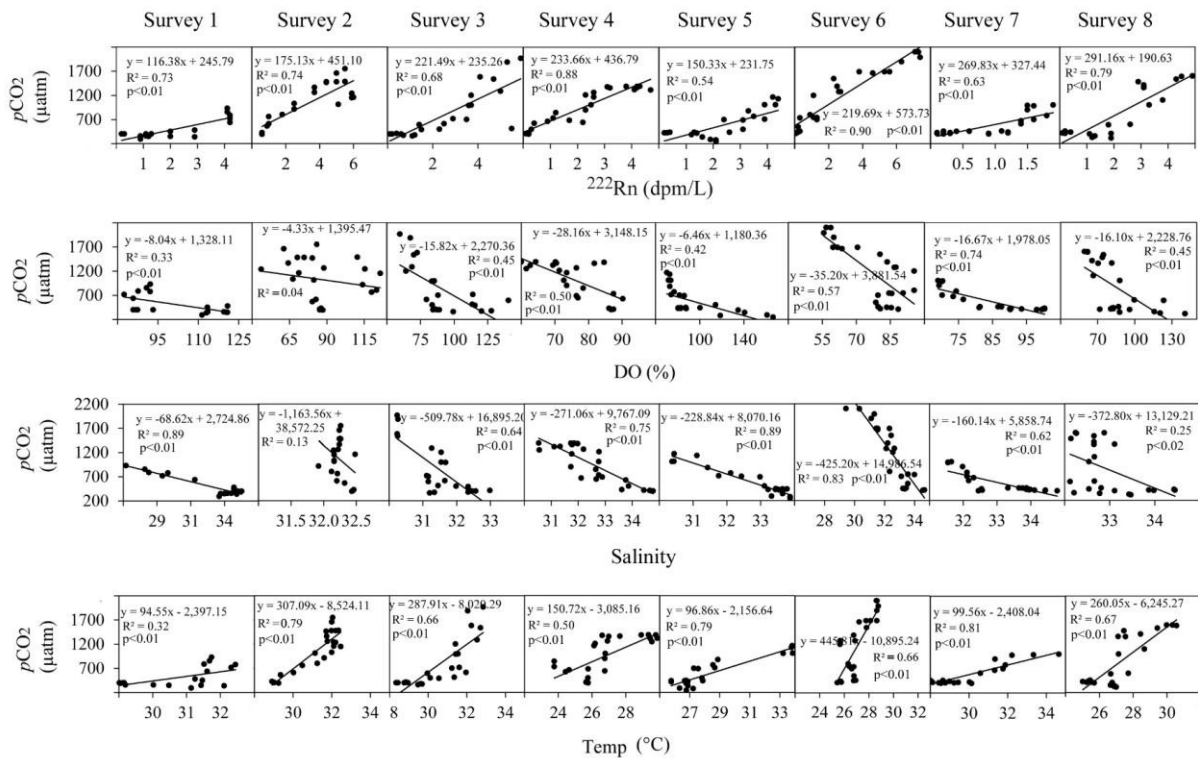


Figure 4. Correlations between  $p\text{CO}_2$  and proxies of potential drivers ( $^{222}\text{Rn}$ , DO, salinity and temperature) during the 8 spatial surveys in Gilimanuk Bay.

Annual rainfall average over the three year sampling span was 695 mm in 2015 (drought year), 1357 mm in 2016 and 1247 mm in 2017, with 2609 mm of rainfall recorded over the 24 months of observations. Historical rainfall for the region is 1316 mm/year. The highest

lagged correlation coefficients (Figure 5) between rainfall and radon, CO<sub>2</sub>, and salinity were used to interpret the lag time between rainfall, groundwater discharge, and subsequent response in groundwater-derived pCO<sub>2</sub> or radon in Gilimanuk Bay. In spite of the relatively dry conditions during sampling, cumulative antecedent rainfall 17 to 63 days prior to surveys had significant correlations to pCO<sub>2</sub> (p≤0.05) with peak correlations (R<sup>2</sup> = 0.81; p<0.002) when 29 days of cumulative rainfall was used. Significant correlations between pCO<sub>2</sub> and cumulative antecedent rainfall was observed 15 and 84 days prior to our survey in the mangrove waters (p<0.05) with the strongest correlation at 48 days cumulative antecedent rainfall (R<sup>2</sup> = 0.90; Figure 5). Correlations in the seagrass area were significant between 29 and 104 days cumulative antecedent rainfall (p<0.05) with the strongest correlation for 73 days of cumulative antecedent rainfall (R<sup>2</sup> = 0.77). This wide range of significant lagged correlations shown may imply that these correlations may not necessarily represent a causation in the seagrass area. Seagrasses and the embayment mouth only showed significant salinity correlations up to 11 days and 4 days, suggesting direct rainfall is the major influence on local salinity. Interestingly, groundwater seepage (as traced by <sup>222</sup>Rn) mimicked pCO<sub>2</sub> in the mangrove forest water, but was decoupled in the highly productive seagrass (Figure 5). This suggests that in-situ productivity was driving pCO<sub>2</sub> rather than groundwater seepage in the seagrasses. In the ocean mouth, <sup>222</sup>Rn had significant correlations with the widest range of delayed rainfall (29-268 days; p<0.05) also implying that these correlations may not necessarily represent a causation in this case. Overall, the lagged correlations imply that delayed groundwater seepage following seasonal rainfall plays a significant role in CO<sub>2</sub> concentration and distribution in this embayment.

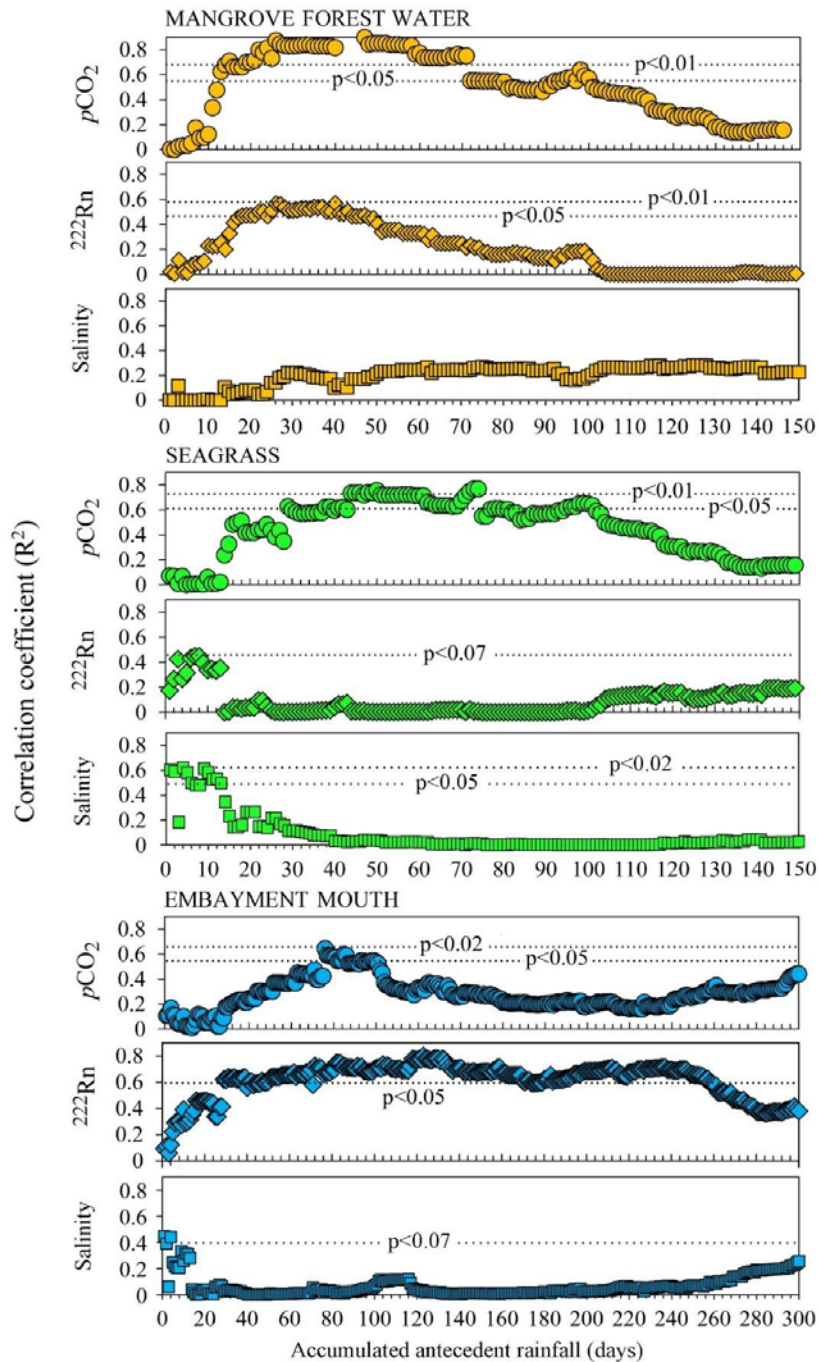


Figure 5. Lagged correlation coefficients ( $R^2$ ) of the relationship between average  $p\text{CO}_2$  (circles),  $^{222}\text{Rn}$  (diamonds) and salinity (squares) and accumulated antecedent rainfall for eight underway surveys in mangrove forest water (brown), seagrass areas (green) and ocean mouth (blue) in Gilimanuk Bay.

$\text{CO}_2$  fluxes revealed shifts from a strong source to the atmosphere in the mangrove forest water, an intermittent sink in the seagrass beds to equilibrium or a weak source at the ocean mouth (Table 3). The total mangrove forest area covered  $\sim 30\%$  of the embayment transect



and seagrass beds covered ~40 %. Measurements suggested that the release of CO<sub>2</sub> to the atmosphere occurred in mangrove forest water (total average CO<sub>2</sub> flux= 18.1 ± 5.8 mmol m<sup>-2</sup> d<sup>-1</sup>) was much greater than in the seagrass beds where the CO<sub>2</sub> flux was 2.5 ± 3.4 mmol m<sup>-2</sup> d<sup>-1</sup>. Seagrass beds were a sink of CO<sub>2</sub> in 2 out of the 8 surveys (Figure 3). Average fluxes along the transect were 9.8 ± 6.0 mmol m<sup>-2</sup> d<sup>-1</sup>, a source of CO<sub>2</sub> (Table 3). No clear seasonal patterns were observed.

Table 3. Average CO<sub>2</sub> fluxes (mmols m<sup>-2</sup> day<sup>-1</sup>) for eight underway surveys categorised into three classes: ocean, seagrass beds and mangrove forest water.

Survey	Ocean	Seagrass	Mangrove
S1	0.0 ± 0.0	-1.3 ± 1.8	10.5 ± 3.2
S2	0.0 ± 0.6	1.8 ± 2.5	22.6 ± 7.6
S3	0.0 ± 0.2	2.1 ± 1.7	16.0 ± 12.4
S4	0.0 ± 1.8	0.3 ± 4.2	18.1 ± 2.2
S5	0.5 ± 0.5	6.3 ± 2.2	11.2 ± 5.7
S6	0.9 ± 0.1	-0.9 ± 3.3	30.1 ± 7.6
S7	0.1 ± 0.0	5.8 ± 1.6	10.7 ± 2.8
S8	0.5 ± 0.2	6.1 ± 10.0	25.8 ± 4.8
Total mean	0.3 ± 0.4	2.5 ± 3.4	18.1 ± 5.8

We selected Raymond and Cole (2001) as the most reasonable k<sub>600</sub> model for the local conditions, and use these values in all figures. Raymond and Cole (2001) estimated k<sub>600</sub> as a function of windspeed using a range of deliberate gas tracer and floating dome experiments in estuaries. Currents were assumed to be a minor driver of k<sub>600</sub> since there was no river inflow and microtides prevented significant current-driven turbulence. Borges et al. (2004) k<sub>600</sub> model resulted in unrealistic high emissions values since their gas transfer velocities estimates were developed in the microtidal Scheldt estuary which experiences strong currents

(Table 3). Wanninkhof (2014) had the lowest values, likely due to this parameterization being developed for the open ocean, where wind is the only driver of near surface turbulence.

Raymond and Cole (2001) presented a mid-range flux value, which is likely more representative of the study site, which does have some tidal flow, but much lower current velocities than the macrotidal Scheldt. Table 4 also includes the oceanic wind speed parameterisations of Wanninkhof and McGillis (1999) and Wanninkhof (2014) for reference.

Table 4. Survey (1-8) and time series, average windspeeds 28 days prior (AWS) and CO<sub>2</sub> flux calculations using four author's transfer velocity parameterizations for equations 2-5: Wanninkhof and McGillis (1999), Raymond and Cole (2001), (Borges et al., 2004) and Wanninkhof (2014), including minimum, maximum, mean, standard deviations.

Survey		CO <sub>2</sub> fluxes (mmol m <sup>-2</sup> d <sup>-1</sup> )				
AWS		W&M99	R&C01	BO4	W2014	Total Mean
Survey 1 2.0 m sec <sup>-1</sup>	Mean	0.1	2.8	6.7	0.8	2.6
	St. Dev ±	0.2	6.4	15.1	1.7	5.9
	Min	-0.1	-3.2	-7.5	-0.9	-2.9
	Max	0.5	16.5	38.9	4.5	15.1
Survey 2 1.6 m sec <sup>-1</sup>	Mean	0.3	16.9	35.8	3.1	14.0
	St. Dev ±	0.2	11.3	26.0	2.3	9.9
	Min	0.0	-0.2	-0.3	0.0	-0.1
	Max	0.7	35.4	81.9	7.1	31.3
Survey 3 1.3 m sec <sup>-1</sup>	Mean	0.1	9.8	21.6	1.5	8.2
	St. Dev ±	0.1	12.4	27.2	1.8	10.4
	Min	0.0	-0.9	-2.0	-0.1	-0.8
	Max	0.4	37.8	83.0	5.6	31.7
Survey 4 0.9 m sec <sup>-1</sup>	Mean	0.1	11.7	21.0	0.9	8.4
	St. Dev ±	0.0	7.4	14.7	0.6	5.7
	Min	0.0	0.0	0.0	0.0	0.0

	Max	0.1	20.0	38.3	1.7	15.0
Survey 5	Mean	0.1	4.3	9.6	0.7	3.7
1.4 m sec <sup>-1</sup>	St. Dev ±	0.1	6.5	14.5	1.1	5.6
	Min	-0.1	-5.1	-11.5	-0.9	-4.4
	Max	0.2	19.6	44.0	3.3	16.8
	1.4 m/s					
Survey 6	Mean	0.4	19.9	44.9	3.4	17.1
1.4 m sec <sup>-1</sup>	St. Dev ±	0.3	13.9	31.2	2.4	11.9
	Min	0.0	1.0	2.2	0.2	0.8
	Max	0.7	41.2	92.5	7.0	35.4
Survey 7	Mean	0.0	3.8	7.6	0.4	3.0
1.1 m sec <sup>-1</sup>	St. Dev ±	0.0	4.8	9.8	0.5	3.8
	Min	0.0	0.0	0.0	0.0	0.0
	Max	0.1	13.3	27.3	1.4	10.5
Survey 8	Mean	0.1	9.8	22.1	1.7	8.4
1.43 m sec <sup>-1</sup>	St. Dev ±	0.3	13.1	29.5	2.2	11.3
	Min	-1.0	-13.1	-28.1	-2.2	-11.1
	Max	0.5	29.0	65.4	5.0	25.0
Time Series	Mean	0.0	1.4	3.1	0.3	1.2
1.5 m sec <sup>-1</sup>	St. Dev ±	0.0	0.4	0.9	0.1	0.3
	Min	0.0	0.6	1.4	0.1	0.5
	Max	0.1	2.7	6.3	0.5	2.4

---

### 3.2 Time Series at the ocean entrance

A 55 hr time series was conducted at the embayment entrance from 16:25, 31 August 2017 to 00:30, 3 September 2017 to investigate aquatic CO<sub>2</sub> exchanges between the embayment and the ocean (Figure 6). There was no precipitation during observations and 11.0 mm of rain was recorded in the month preceding the time series observations. Water temperatures ranged

from 25.1 to 27.7 °C and were lowest between midnight and early morning. Salinity ranged from 34.9 to 35.2. The higher salinity measurements on the outgoing tide may be a result of evaporation within this shallow embayment (data not shown). DO ranged from 82.5 % to 104.3 %. In spite of some data gaps, DO appeared to have diel trends reflecting photosynthesis during the day and respiration at night (Figure 7). The  $p\text{CO}_2$  trends did not follow DO. Indeed,  $p\text{CO}_2$  had stronger correlations to  $^{222}\text{Rn}$  than DO during the day (Figure 7) implying the groundwater  $\text{CO}_2$  source was stronger than the photosynthesis sink.  $^{222}\text{Rn}$  followed a tidal cycle and correlated with  $p\text{CO}_2$  during both incoming and outgoing tides ( $R^2=0.53$  &  $R^2=0.22$ , respectively; data not shown). The highest  $^{222}\text{Rn}$ , salinity and  $\text{CO}_2$  values were observed during the two lowest tides (overall tidal range = 1.5m) which is consistent with groundwater-derived inputs that are well known to occur at low tide (Atkins et al., 2013; Call et al., 2015; McMahan & Santos, 2017; Santos et al., 2009). It is difficult to explain the increase in  $p\text{CO}_2$  from ~440 to 500  $\mu\text{atm}$  in the last 4 hours of the time series since both radon (groundwater proxy) and DO (respiration proxy) had no similar changes.  $p\text{CO}_2$  was above atmospheric equilibrium throughout with the highest  $p\text{CO}_2$  observations at low tides and lowest at high tides. Low  $p\text{CO}_2$  at the embayment mouth are consistent with the survey observations of  $\text{CO}_2$  outgassing and/or uptake by the seagrass beds (Table 4; R&C01:  $1.4 \pm 0.4 \text{ mmol m}^{-2} \text{ d}^{-1}$ ).

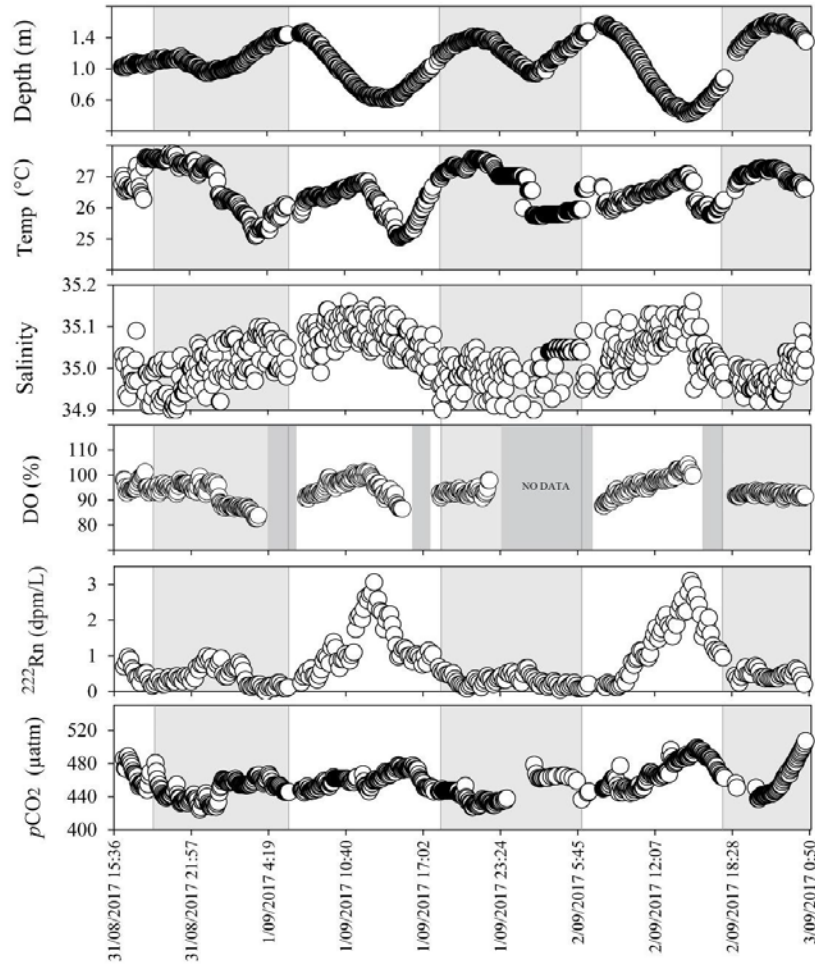


Figure 6. Observations during the 55 hour time series conducted at the ocean mouth of Gilimanuk Bay.

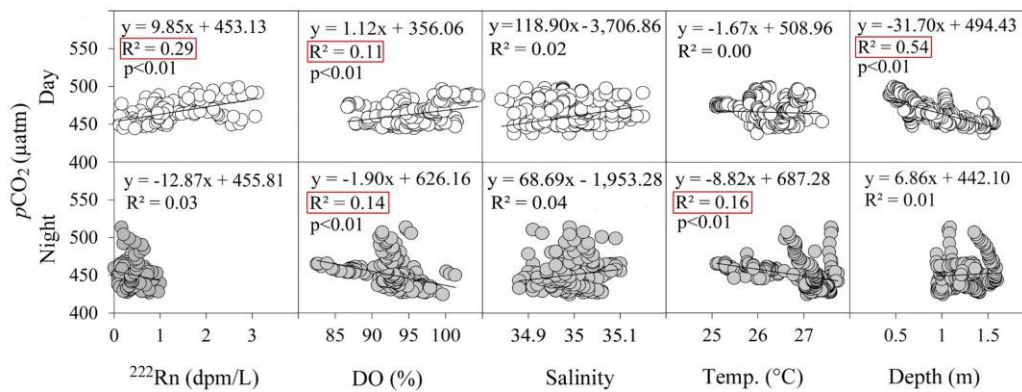


Figure 7. Correlations between  $p\text{CO}_2$  and ancillary variables during the 55 hour time series conducted at the ocean mouth of Gilimanuk Bay during daytime (white circles) and night time (grey circles).

#### 4. Discussion

Aquatic systems in Southeast Asia are recognised as significant sources of  $\text{CO}_2$  to the atmosphere but remain poorly represented in global databases (Müller et al., 2015). The few studies available focus on tropical river-dominated estuaries which produce significant  $\text{CO}_2$  fluxes (Borges & Abril, 2011; Müller et al., 2015). Global summaries of water-to-air  $\text{CO}_2$  fluxes are generally confined to human impacted river-dominated estuarine systems (Cai, 2011). A recent study in a temperate autotrophic marine dominated system in Australia reported ten-fold lower and reversed  $\text{CO}_2$  fluxes than the more studied river-dominated counterparts (Maher & Eyre, 2012). Since there is a paucity of data from marine-dominated tropical coastal embayments, our investigation contributes to filling gaps in global estuarine  $\text{CO}_2$  fluxes.

By categorizing  $\text{CO}_2$  fluxes into three classes (mangrove forest water, seagrass beds and the ocean-dominated mouth), comparisons with temperate coastal water  $\text{CO}_2$  fluxes could be made. For instance, mangrove forest water had  $\text{CO}_2$  fluxes ( $18.1 \pm 5.8 \text{ mmol m}^{-2} \text{ d}^{-1}$ ) similar to estuarine systems such as the York River estuary in the U.S.A. ( $17 \text{ mmol m}^{-2} \text{ d}^{-1}$ ) (Raymond et al., 2000) and the Pearl River in China ( $24 \text{ mmol m}^{-2} \text{ d}^{-1}$ ) (Yuan et al., 2011). Overall, the mangrove forest water dominated surrounding water  $\text{CO}_2$  fluxes and were within estimated flux ranges for many global coastal waters (Chen et al., 2013). A study by Ho et al. (2017) reported average  $\text{CO}_2$  fluxes of  $105 \pm 9$  and  $99 \pm 6 \text{ mmol m}^{-2} \text{ d}^{-1}$  at the end of the wet

season, where  $p\text{CO}_2$  values ranged from 1000 to 6200  $\mu\text{atm}$  (present study ranges = 516 (S1; Nov.2015) to 1164  $\mu\text{atm}$  (S6; Jan. 2017; Table 2). We report overall embayment  $\text{CO}_2$  fluxes of  $9.8 \pm 6.0 \text{ mmol m}^{-2} \text{ d}^{-1}$  comparable to the lower range of the Everglades study, estimated global mangrove fluxes of 4.6 to 113.5  $\text{mmol m}^{-2} \text{ d}^{-1}$  (Borges et al., 2003) and revised global estimates of  $56.8 \pm 8.9 \text{ mmol m}^{-2} \text{ d}^{-1}$  (Rosentreter et al., 2018). This is most likely due to lack of river inputs and large uptake by seagrass beds in the mid-embayment.

Seasonality seems to play a greater role in temperate waters (Guo et al., 2009). In the Changjiang Estuary (China) seasonal ranges were 52.9  $\text{mmol m}^{-2} \text{ d}^{-1}$  (December) to 92.9  $\text{mmol m}^{-2} \text{ d}^{-1}$  (August) based on the parameterization of Raymond and Cole (2001) (Zhai et al., 2007). Seasonality was not observed throughout our study. Gilimanuk Bay  $\text{CO}_2$  emissions ranged from 2.8  $\text{mmol m}^{-2} \text{ d}^{-1}$  (S1; October 2015) to 16.9  $\text{mmol m}^{-2} \text{ d}^{-1}$  (S2; January 2016; Table 4) with no clear changes over an annual temperature cycle. Autotrophic coastal systems have been reported as sinks of atmospheric derived  $\text{CO}_2$  (Borges and Abril, 2011; Maher and Eyre, 2012). The seagrass-dominated area of Gilimanuk Bay alternated between a  $\text{CO}_2$  source and sink. The more consistent  $\text{CO}_2$  source in the near shore ocean was possibly due to coral calcification in Gilimanuk Bay's fringing coral reefs (Figure 8).

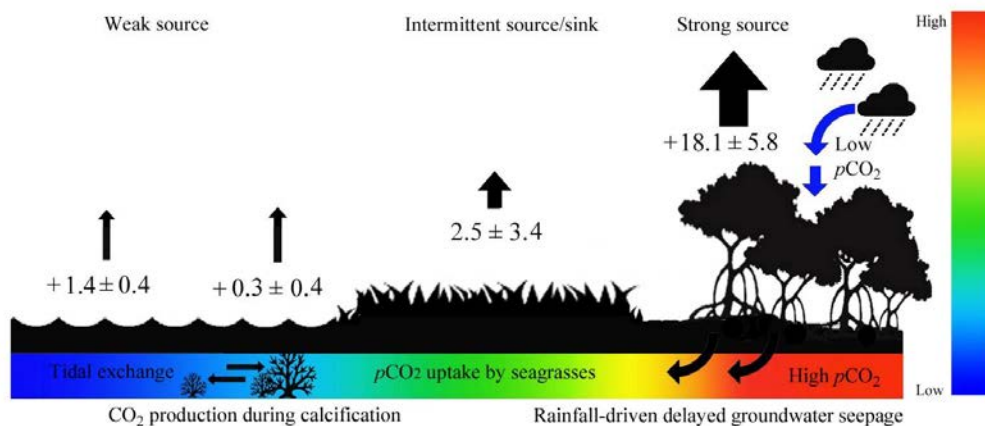


Figure 8. Conceptual model summarizing water-to-air CO<sub>2</sub> (mmols m<sup>-2</sup> d<sup>-1</sup>) along the transect investigated. The gradient bar (right) indicates high to low *p*CO<sub>2</sub> fluxes and the different size black arrows highlight the ratio of fluxes between each habitat.

Groundwater seepage, porewater exchange and rainfall events have been linked to delayed groundwater discharge as a source of CO<sub>2</sub> in subtropical systems (Ruiz-Halpern et al., 2015). Rainfall, particularly flood events, rapidly transport carbon stored in upper soil profiles across the land-to-water interface (Atkins et al., 2013; Gatland et al., 2014; Jeffrey et al., 2016; Webb et al., 2016). Paquay et al. (2007) reported that water residence times and periodic floods drove the distribution of *p*CO<sub>2</sub> in Hilo Bay (Hawaii) with groundwater seepage suggested to explain a 3 day delay of elevated *p*CO<sub>2</sub> after a heavy rainfall event. In contrast to Hilo Bay, Gilimanuk Bay has no riverine input, making groundwater seepage a dominant source of CO<sub>2</sub> year-round (average R<sup>2</sup>=0.74) followed by temperature (average R<sup>2</sup>=0.65) and salinity (average R<sup>2</sup>=0.63; Figure 4).

Tidally-driven porewater exchange (tidal pumping) has been suggested to release carbon dioxide and nutrients to estuaries (Sadat-Noori et al., 2016) and intertidal flats (Bouillon, Connolly, et al., 2008; Santos et al., 2014). Large tidal amplitudes (spring tides) have been related to enhanced <sup>222</sup>Rn in coastal waters as observed off a sandy beach in Korea (Kim & Hwang, 2002) and in Florida (Santos et al., 2009) and mangrove forest water in Australia (Call et al., 2015). Radon traces any water in contact with sediments regardless of salinity. However, our dataset cannot resolve whether tidally-driven porewater exchange or fresh groundwater discharge are the source of radon enrichments in the mangrove forest water. Considering the small tidal amplitude, lack of well-defined tidal creeks in the mangroves, steep topography surrounding the upper embayment, and the significant correlations between radon and antecedent rainfall, we suggest that delayed fresh groundwater discharge (rather



than tidal pumping) is more likely to be the radon and CO<sub>2</sub> source to the upper embayment. . Groundwater discharge at the shoreline is well known to lag rainfall for several months. Seasonal oscillation in groundwater level and inland recharge can explain large saline groundwater discharge several months after rainfall as observed in a Massachusetts aquifer (Michael et al., 2005). Unfortunately, no groundwater level data are available for the Gilimanuk Bay area to build on this hypothesis.

CO<sub>2</sub> derived from the mangrove forest in the upper embayment appears to be fixed by seagrass beds in the lower embayment, intermittently transforming the lower embayment into a net sink of CO<sub>2</sub> (Figure 1; Figure 3; Figure 8). However, there was higher *p*CO<sub>2</sub> and water-to-air *p*CO<sub>2</sub> fluxes in wetter periods in the seagrass beds (Figure 9; Surveys 3, 6 & 8) which coincided with the highest antecedent rainfall (Table 3). Seagrasses, although known to be net autotrophic, are largely under-represented in global carbon budgets (Duarte et al., 2010). Additionally, there are large uncertainties in the extent of seagrass beds globally, resulting from a) many regions in Indonesia being known to support extensive seagrass beds but have not been surveyed and b) the continuing loss of seagrass bed areas as a result of well-reported anthropogenic degradation (Alongi et al., 2016; Duarte et al., 2010; Unsworth & Cullen, 2010).

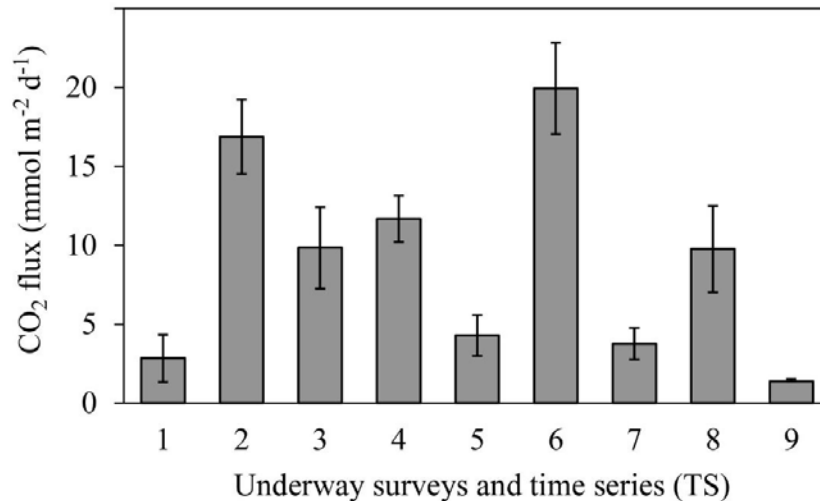


Figure 9. Average water-to-air CO<sub>2</sub> fluxes using piston velocities from the parameterization of Raymond and Cole (2001) for eight underway surveys and time series conducted in Gilimanuk Bay.

The ocean's blue carbon sinks (mangroves, saltmarshes and seagrasses) capture and store approximately 70% of the carbon perpetually stored in aquatic systems (Nellemann & Corcoran, 2009). In contrast to mangrove forests habitats, which occur only in warmer tropical and subtropical climates, seagrasses are also present in colder northern and southern latitudes (Orth et al., 2006). The importance of their combined presence with mangrove forests in tropical systems is noteworthy as both mangrove forests and seagrass beds stabilise sediment (Hogarth, 2015). About 50% of net primary production produced by seagrasses is buried within seagrass sediments (Kennedy et al., 2010), and ~ 8% of mangrove net primary production is retained in mangrove forest soils (Bouillon, Borges, et al., 2008).

Degradation or loss of mangrove forests and seagrass beds may cause the release of large stores of sedimentary carbon to both the atmosphere and the coastal ocean (McLeod et al.,

2011). Therefore, continued degradation may increase atmospheric CO<sub>2</sub>. Due to the high carbon stores in blue carbon systems, and in particular with the tropical regions such as Indonesia, prevention of ecosystem degradation is crucial for limiting the potential release of this carbon to the atmosphere as CO<sub>2</sub> (Tollefson, 2018). Strategies to counter the drainage of blue carbon ecosystems would be an effective measure in maintaining carbon in soils (Crooks et al., 2011). For example, construction of artificial canals draining coastal wetlands more than doubled CO<sub>2</sub> emissions from waterways on the highly urbanized Gold Coast, Australia (Macklin et al., 2014). Our investigation further demonstrates the role seagrass beds play in taking up dissolved inorganic carbon and preventing emissions from groundwater-derived CO<sub>2</sub> in nearby ecosystems.

## **5. Conclusion**

Our investigations across a coral reef-seagrass-mangrove continuum revealed a CO<sub>2</sub> source in the mangrove dominated upper bay apparently associated with delayed groundwater inputs, and differing CO<sub>2</sub> dynamics in the lower bay driven by the uptake of CO<sub>2</sub> by seagrass. The bay mouth was a source of CO<sub>2</sub> possibly due to production of CO<sub>2</sub> during fringing coral reef calcification. The average CO<sub>2</sub> water-to-air flux along the transect was  $9.8 \pm 6.0 \text{ mmol m}^{-2} \text{ d}^{-1}$ . Antecedent rainfall and radon were the best predictors of CO<sub>2</sub> dynamics, with no clear seasonality observed, in contrast to better studied seasonal temperate systems. Potential changes in rainfall events due to climate change in Indonesia (Overpeck & Cole, 2007) as well as ecosystem degradation may alter aquatic CO<sub>2</sub> emissions. This study may assist when determining anthropogenic modification buffer zones in mangrove forest embayments. As *p*CO<sub>2</sub> data in tropical coastal embayments are scarce, more studies are needed to assess the role of these systems in the global carbon cycle.

## **Acknowledgements**

Paul Macklin was funded by the Australian Government Research Training Program Scholarship. We acknowledge Ceylena Holloway from the National Marine Science Centre for support with research instrumentation. The Ministry of Research, Technology and Higher Education of the Republic of Indonesia (RISTEKDIKTI); The Ministry of Home Affairs of the Republic of Indonesia (MoHA); the Direktorat Jenderal Sumber Daya Air and Governor of Bali I Made Mangku Pastika are acknowledged for access and permissions to sample. We acknowledge support from the Australian Research Council (DE140101733, DE150100581, and LE120100156) that partially funded IRS and DTM salaries and the portable analytical instrumentation.

## References

- Alongi, D., Murdiyarso, D., Fourqurean, J., Kauffman, J., Hutahaean, A., Crooks, S., . . . Fortes, M. (2016). Indonesia's blue carbon: a globally significant and vulnerable sink for seagrass and mangrove carbon. *Wetlands Ecology and Management*, *24*(1), 3-13.
- Atkins, M. L., Santos, I. R., Ruiz-Halpern, S., & Maher, D. T. (2013). Carbon dioxide dynamics driven by groundwater discharge in a coastal floodplain creek. *Journal of Hydrology*, *493*, 30-42.
- Atwood, T. B., Connolly, R. M., Almahasheer, H., Carnell, P. E., Duarte, C. M., Lewis, C. J. E., . . . Macreadie, P. I. (2017). Global patterns in mangrove soil carbon stocks and losses. *Nature Climate Change*, *7*(7), 523.
- Borges, A., & Abril, G. (2011). 5.04-Carbon dioxide and methane dynamics in estuaries. *Treatise on Estuarine and Coastal Science, Volume 5: Biogeochemistry*, 119-161.
- Borges, A., Djenidi, S., Lacroix, G., Théate, J., Delille, B., & Frankignoulle, M. (2003). Atmospheric CO<sub>2</sub> flux from mangrove surrounding waters. *Geophysical Research Letters*, *30*(11).
- Borges, A. V., Delille, B., Schiettecatte, L. S., Gazeau, F., Abril, G., & Frankignoulle, M. (2004). Gas transfer velocities of CO<sub>2</sub> in three European estuaries (Randers Fjord, Scheldt, and Thames). *Limnology and Oceanography*, *49*(5), 1630-1641.
- Bouillon, S., Borges, A. V., Castañeda-Moya, E., Diele, K., Dittmar, T., Duke, N. C., . . . Middelburg, J. J. (2008). Mangrove production and carbon sinks: a revision of global budget estimates. *Global Biogeochemical Cycles*, *22*(2).
- Bouillon, S., Connolly, R., & Lee, S. (2008). Organic matter exchange and cycling in mangrove ecosystems: recent insights from stable isotope studies. *Journal of Sea Research*, *59*(1-2), 44-58.
- Bouillon, S., Middelburg, J. J., Dehairs, F., Borges, A. V., Abril, G., Flindt, M. R., . . . Kristensen, E. (2007). Importance of intertidal sediment processes and porewater

- exchange on the water column biogeochemistry in a pristine mangrove creek (Ras Dege, Tanzania). *Biogeosciences Discussions*, 4(1), 317-348.
- Cai, W.-J. (2011). Estuarine and coastal ocean carbon paradox: CO<sub>2</sub> sinks or sites of terrestrial carbon incineration? *Annual Review of Marine Science*, 3, 123-145.
- Call, M., Maher, D. T., Santos, I. R., Ruiz-Halpern, S., Mangion, P., Sanders, C. J., . . . Murray, R. (2015). Spatial and temporal variability of carbon dioxide and methane fluxes over semi-diurnal and spring–neap–spring timescales in a mangrove creek. *Geochimica et Cosmochimica Acta*, 150, 211-225.
- Chen, C.-T., Huang, T.-H., Chen, Y.-C., Bai, Y., He, X., & Kang, Y. (2013). Air-sea exchanges of CO<sub>2</sub> in the world's coastal seas. *Biogeosciences*, 10(10), 6509.
- Chen, X.; Zhang, F., Lao, Y., Wang, X., Du, J., Santos, I. R. (2018). Submarine Groundwater Discharge-Derived Carbon Fluxes in Mangroves: An Important Component of Blue Carbon Budgets? *Journal of Geophysical Research: Oceans* doi.org/10.1029/2018JC014448.
- Crooks, S., Herr, D., Tamelander, J., Laffoley, D., & Vandever, J. (2011). Mitigating climate change through restoration and management of coastal wetlands and near-shore marine ecosystems: challenges and opportunities.
- Dittmar, T., Koch, B., & Jaffé, R. (2009). Tools for studying biogeochemical connectivity among tropical coastal ecosystems *Ecological Connectivity among Tropical Coastal Ecosystems* (pp. 425-455): Springer.
- Donato, D. C., Kauffman, J. B., Murdiyarso, D., Kurnianto, S., Stidham, M., & Kanninen, M. (2011). Mangroves among the most carbon-rich forests in the tropics. *Nature Geoscience*, 4(5), 293.
- Duarte, C. M., & Cebrian, J. (1996). The fate of marine autotrophic production. *Limnology and Oceanography*, 41(8), 1758-1766.
- Duarte, C. M., Marbà, N., Gacia, E., Fourqurean, J. W., Beggins, J., Barrón, C., & Apostolaki, E. T. (2010). Seagrass community metabolism: Assessing the carbon sink capacity of seagrass meadows. *Global Biogeochemical Cycles*, 24(4).
- Dulaiova, H., Peterson, R., Burnett, W., & Lane-Smith, D. (2005). A multi-detector continuous monitor for assessment of <sup>222</sup>Rn in the coastal ocean. *Journal of Radioanalytical and Nuclear Chemistry*, 263(2), 361-363.
- Fourqurean, J. W., Zieman, J. C., & Powell, G. V. (1992). Phosphorus limitation of primary production in Florida Bay: evidence from C: N: P ratios of the dominant seagrass *Thalassia testudinum*. *Limnology and Oceanography*, 37(1), 162-171.
- Ganguly, D., Singh, G., Ramachandran, P., Selvam, A. P., Banerjee, K., & Ramachandran, R. (2017). Seagrass metabolism and carbon dynamics in a tropical coastal embayment. *Ambio*, 46(6), 667-679.
- Gatland, J. R., Santos, I. R., Maher, D. T., Duncan, T., & Erler, D. V. (2014). Carbon dioxide and methane emissions from an artificially drained coastal wetland during a flood: Implications for wetland global warming potential. *Journal of Geophysical Research: Biogeosciences*, 119(8), 1698-1716.
- Giri, C., Ochieng, E., Tieszen, L. L., Zhu, Z., Singh, A., Loveland, T., . . . Duke, N. (2011). Status and distribution of mangrove forests of the world using earth observation satellite data. *Global Ecology and Biogeography*, 20(1), 154-159.

- Green, E., & Short, F. (2003). World Atlas of Seagrasses. Prepared by the UNEP World Conservation Monitoring Centre. *University of California, Press Berkeley, USA*.
- Greenberg, R., Maldonado, J. E., Droege, S., & McDonald, M. (2006). Tidal marshes: a global perspective on the evolution and conservation of their terrestrial vertebrates. *Bioscience*, *56*(8), 675-685.
- Guannel, G., Arkema, K., Ruggiero, P., & Verutes, G. (2016). The power of three: Coral reefs, seagrasses and mangroves protect coastal regions and increase their resilience. *PloS one*, *11*(7), e0158094.
- Guo, X., Dai, M., Zhai, W., Cai, W. J., & Chen, B. (2009). CO<sub>2</sub> flux and seasonal variability in a large subtropical estuarine system, the Pearl River Estuary, China. *Journal of Geophysical Research: Biogeosciences*, *114*(G3).
- Hemminga, M., Slim, F., Kazungu, J., Ganssen, G., Nieuwenhuize, J., & Kruyt, N. (1994). Carbon outwelling from a mangrove forest with adjacent seagrass beds and coral reefs (Gazi Bay, Kenya). *Marine Ecology Progress Series*, 291-301.
- Hemminga, M. A., & Duarte, C. M. (2000). *Seagrass Ecology*: Cambridge University Press.
- Ho, D. T., Ferrón, S., Engel, V. C., Anderson, W. T., Swart, P. K., Price, R. M., & Barbero, L. (2017). Dissolved carbon biogeochemistry and export in mangrove-dominated rivers of the Florida Everglades. *Biogeosciences*, *14*(9), 2543-2559.
- Hogarth, P. J. (2015). *The biology of mangroves and seagrasses*: Oxford University Press.
- Jeffrey, L. C., Maher, D. T., Santos, I. R., McMahon, A., & Tait, D. R. (2016). Groundwater, Acid and Carbon Dioxide Dynamics Along a Coastal Wetland, Lake and Estuary Continuum. *Estuaries and Coasts*, *39*(5), 1325.
- Jennerjahn, T. C., & Ittekkot, V. (2002). Relevance of mangroves for the production and deposition of organic matter along tropical continental margins. *Naturwissenschaften*, *89*(1), 23-30.
- Kennedy, H., Beggins, J., Duarte, C. M., Fourqurean, J. W., Holmer, M., Marbà, N., & Middelburg, J. J. (2010). Seagrass sediments as a global carbon sink: Isotopic constraints. *Global Biogeochemical Cycles*, *24*(4).
- Kim, G., & Hwang, D. W. (2002). Tidal pumping of groundwater into the coastal ocean revealed from submarine 222Rn and CH<sub>4</sub> monitoring. *Geophysical Research Letters*, *29*(14), 23-21-23-24.
- Macklin, P. A., Maher, D. T., & Santos, I. R. (2014). Estuarine canal estate waters: Hotspots of CO<sub>2</sub> outgassing driven by enhanced groundwater discharge? *Marine Chemistry*, *167*, 82-92.
- Maher, D., & Eyre, B. (2012). Carbon budgets for three autotrophic Australian estuaries: Implications for global estimates of the coastal air-water CO<sub>2</sub> flux. *Global Biogeochemical Cycles*, *26*(1).
- Maher, D. T., Santos, I. R., Golsby-Smith, L., Gleeson, J., & Eyre, B. D. (2013). Groundwater-derived dissolved inorganic and organic carbon exports from a mangrove tidal creek: The missing mangrove carbon sink? *Limnology and Oceanography*, *58*(2), 475-488.
- Maher, D. T., Santos, I. R., Schulz, K. G., Call, M., Jacobsen, G. E., & Sanders, C. J. (2017). Blue carbon oxidation revealed by radiogenic and stable isotopes in a mangrove system. *Geophysical Research Letters*, *44*, 4889-4896.

- Marbawa, I. K. C., Astarini, I. A., & Mahardika, I. G. (2015). Analisis Vegetasi Mangrove Untuk Strategi Pengelolaan Ekosistem Berkelanjutan di Taman Nasional Bali Barat. *ECOTROPHIC: Jurnal Ilmu Lingkungan (Journal of Environmental Science)*, 8(1), 24-38.
- McLeod, E., Chmura, G. L., Bouillon, S., Salm, R., Björk, M., Duarte, C. M., . . . Silliman, B. R. (2011). A blueprint for blue carbon: toward an improved understanding of the role of vegetated coastal habitats in sequestering CO<sub>2</sub>. *Frontiers in Ecology and the Environment*, 9(10), 552-560.
- McMahon, A., & Santos, I. R. (2017). Nitrogen enrichment and speciation in a coral reef lagoon driven by groundwater inputs of bird guano. *Journal of Geophysical Research: Oceans*, 122(9), 7218-7236.
- Michael, H. A., Mulligan, A. E., & Harvey, C. F. (2005). Seasonal oscillations in water exchange between aquifers and the coastal ocean. *Nature*, 436(7054), 1145.
- Müller, D., Warneke, T., Rixen, T., Müller, M., Mujahid, A., Bange, H., & Notholt, J. (2015). Fate of peat-derived carbon and associated CO<sub>2</sub> and CO emissions from two Southeast Asian estuaries. *Biogeosciences Discussions*, 12(21).
- Murdiyarmo, D., Purbopuspito, J., Kauffman, J. B., Warren, M. W., Sasmito, S. D., Donato, D. C., . . . Kurnianto, S. (2015). The potential of Indonesian mangrove forests for global climate change mitigation. *Nature Climate Change*, 5(12), 1089.
- Nellemann, C., & Corcoran, E. (2009). *Blue carbon: the role of healthy oceans in binding carbon: a rapid response assessment*: UNEP/Earthprint.
- Ningsih, N. S., Rakhmaputeri, N., & Harto, A. B. (2013). Upwelling variability along the southern coast of Bali and in Nusa Tenggara waters. *Ocean Science Journal*, 48(1), 49-57.
- Orth, R. J., Carruthers, T. J., Dennison, W. C., Duarte, C. M., Fourqurean, J. W., Heck, K. L., . . . Olyarnik, S. (2006). A global crisis for seagrass ecosystems. *Bioscience*, 56(12), 987-996.
- Overpeck, J. T., & Cole, J. E. (2007). Climate change: Lessons from a distant monsoon. *Nature*, 445(7125), 270.
- Paquay, F. S., Mackenzie, F. T., & Borges, A. V. (2007). Carbon dioxide dynamics in rivers and coastal waters of the “big island” of Hawaii, USA, during baseline and heavy rain conditions. *Aquatic Geochemistry*, 13(1), 1-18.
- Pierrot, D., Neill, C., Sullivan, K., Castle, R., Wanninkhof, R., Lüger, H., . . . Cosca, C. E. (2009). Recommendations for autonomous underway pCO<sub>2</sub> measuring systems and data-reduction routines. *Deep Sea Research Part II: Topical Studies in Oceanography*, 56(8-10), 512-522.
- Purbo-Hadiwidjojo, M. (1971). Geological map of Bali 1: 250,000. *Geological Survey of Indonesia Publication*.
- Purnomo, H. K., Yusniawati, Y., Putrika, A., Hanayani, W., & Yasman, Y. (2017). *Seagrass species diversity at various seagrass bed ecosystems in the West Bali National Park Area*. Paper presented at the Prosiding Seminar Nasional Masyarakat Biodiversitas Indonesia.

- Raymond, P. A., Bauer, J. E., & Cole, J. J. (2000). Atmospheric CO<sub>2</sub> evasion, dissolved inorganic carbon production, and net heterotrophy in the York River estuary. *Limnology and Oceanography*, 45(8), 1707-1717.
- Raymond, P. A., & Cole, J. J. (2001). Gas exchange in rivers and estuaries: Choosing a gas transfer velocity. *Estuaries and Coasts*, 24(2), 312-317.
- Robertson, A., Alongi, D., & Boto, K. (1992). Food chains and carbon fluxes. *Tropical Mangrove Ecosystems*, 293-326.
- Rosentreter, J. A., Maher, D., Erler, D., Murray, R., & Eyre, B. (2018). Seasonal and temporal CO<sub>2</sub> dynamics in three tropical mangrove creeks—A revision of global mangrove CO<sub>2</sub> emissions. *Geochimica et Cosmochimica Acta*, 222, 729-745.
- Ruiz-Halpern, S., Maher, D. T., Santos, I. R., & Eyre, B. D. (2015). High CO<sub>2</sub> evasion during floods in an Australian subtropical estuary downstream from a modified acidic floodplain wetland. *Limnology and Oceanography*, 60(1), 42-56.
- Sadat-Noori, M., Maher, D. T., & Santos, I. R. (2016). Groundwater discharge as a source of dissolved carbon and greenhouse gases in a subtropical estuary. *Estuaries and Coasts*, 39(3), 639-656.
- Santos, I. R., Bryan, K. R., Pilditch, C. A., & Tait, D. R. (2014). Influence of porewater exchange on nutrient dynamics in two New Zealand estuarine intertidal flats. *Marine Chemistry*, 167, 57-70.
- Santos, I. R., Burnett, W. C., Dittmar, T., Suryaputra, I. G., & Chanton, J. (2009). Tidal pumping drives nutrient and dissolved organic matter dynamics in a Gulf of Mexico subterranean estuary. *Geochimica et Cosmochimica Acta*, 73(5), 1325-1339.
- Santos, I. R., Maher, D. T., & Eyre, B. D. (2012). Coupling automated radon and carbon dioxide measurements in coastal waters. *Environmental Science & Technology*, 46(14), 7685-7691.
- Scott, D. B., Frail-Gauthier, J., & Mudie, P. J. (2014). *Coastal wetlands of the world: geology, ecology, distribution and applications*: Cambridge University Press.
- Short, F., Carruthers, T., Dennison, W., & Waycott, M. (2007). Global seagrass distribution and diversity: a bioregional model. *Journal of Experimental Marine Biology and Ecology*, 350(1-2), 3-20.
- Signa, G., Mazzola, A., Kairo, J., & Vizzini, S. (2017). Small-scale variability in geomorphological settings influences mangrove-derived organic matter export in a tropical bay. *Biogeosciences*, 14(3), 617.
- Sippo, J. Z., Maher, D. T., Tait, D. R., Ruiz-Halpern, S., Sanders, C. J., & Santos, I. R. (2017). Mangrove outwelling is a significant source of oceanic exchangeable organic carbon. *Limnology and Oceanography Letters*, 2(1), 1-8.
- Siswanto, S. (2008). Seasonal Pattern of Wind Induced Upwelling over Java–Bali Sea Waters and Surrounding Area. *International Journal of Remote Sensing and Earth Sciences (IJReSES)*, 5.
- Spalding, M., Blasco, F., & Field, C. (1997). World mangrove atlas.
- Tait, D. R., Maher, D. T., Macklin, P. A., & Santos, I. R. (2016). Mangrove pore water exchange across a latitudinal gradient. *Geophysical Research Letters*, 43(7), 3334-3341.



- Thoha, H. (2007). Kelimpahan plankton di ekosistem perairan Teluk Gilimanuk, Taman Nasional, Bali Barat. *Makara, Sains*, 11(1), 44-48.
- Tollefson, J. (2018). Climate scientists unlock secrets of 'blue carbon'. *Nature*, 553(7687), 139-140.
- Torres-Pulliza, D., Wilson, J. R., Darmawan, A., Campbell, S. J., & Andréfouët, S. (2013). Ecoregional scale seagrass mapping: A tool to support resilient MPA network design in the Coral Triangle. *Ocean & Coastal Management*, 80, 55-64.
- Unsworth, R. K., & Cullen, L. C. (2010). Recognising the necessity for Indo-Pacific seagrass conservation. *Conservation Letters*, 3(2), 63-73.
- Unsworth, R. K., De León, P. S., Garrard, S. L., Jompa, J., Smith, D. J., & Bell, J. J. (2008). High connectivity of Indo-Pacific seagrass fish assemblages with mangrove and coral reef habitats. *Marine Ecology Progress Series*, 353, 213-224.
- Utama, R. (2015). Positioning of Eco Tourism Objects in Bali Indonesia. Available at SSRN 2595139.
- Wanninkhof, R. (2014). Relationship between wind speed and gas exchange over the ocean revisited. *Limnology and Oceanography: Methods*, 12(6), 351-362.
- Wanninkhof, R., & McGillis, W. R. (1999). A cubic relationship between air-sea CO<sub>2</sub> exchange and wind speed. *Geophysical Research Letters*, 26(13), 1889-1892.
- Webb, J. R., Santos, I. R., Tait, D. R., Sippo, J. Z., Macdonald, B. C., Robson, B., & Maher, D. T. (2016). Divergent drivers of carbon dioxide and methane dynamics in an agricultural coastal floodplain: Post-flood hydrological and biological drivers. *Chemical Geology*, 440, 313-325.
- Weiss, R. F. (1974). Carbon dioxide in water and seawater: the solubility of a non-ideal gas. *Marine Chemistry*, 2(3), 203-215.
- Yuan, X.-C., Yin, K., Cai, W.-J., Ho, A., Xu, J., & Harrison, P. J. (2011). Influence of seasonal monsoons on net community production and CO<sub>2</sub> in subtropical Hong Kong coastal waters. *Biogeosciences*, 8(2), 289-300.
- Zhai, W., Dai, M., & Guo, X. (2007). Carbonate system and CO<sub>2</sub> degassing fluxes in the inner estuary of Changjiang (Yangtze) River, China. *Marine Chemistry*, 107(3), 342-356.
- Zulkarnaen, A. R., Putri, A. N., & Sobari, I. (2014). Studi Komunitas Lamun di Perairan Teluk Gilimanuk dan Labuhan Lalang, Taman Nasional Bali Barat. *Prosiding PIT X ISOI 2013*, 1(1).

## Highlights

- An aquatic CO<sub>2</sub> source in the mangrove dominated upper embayment waters was associated with delayed groundwater inputs
- A shifting CO<sub>2</sub> source-sink in the lower embayment bay was driven by the uptake of CO<sub>2</sub> by seagrass and mixing with oceanic waters
- This more pristine system differs to modified landscapes, where potential uptake of CO<sub>2</sub> is weakened due to the degradation of seagrass beds, or emissions are increased due to drainage of coastal wetlands.
- Antecedent rainfall and radon were found to be the best predictors of CO<sub>2</sub> dynamics, with no clear seasonality observed, in contrast to better studied seasonal temperate systems.
- Extended delays of groundwater-derived CO<sub>2</sub> in the coastal waters compared to mangrove forest waters highlight the importance of comparative studies with more modified systems which are known to have more rapid delivery of carbon to coastal waters.
- This study may assist when determining anthropogenic modification buffer zones in mangrove forest embayments.